Interactions Between Heterogeneous Surfaces of Polymers and Water

H. MURASE,* K. NANISHI, H. KOGURE, T. FUJIBAYASHI, K. TAMURA,* and N. HARUTA

Research Laboratory of Kansai Paint Co., Ltd., 4-17-1, Higashiyawata, Hiratsuka-city, Kanagawa-prefecture 254, Japan

SYNOPSIS

Preliminary investigations for the interactions between surfaces of polymers and water were conducted by the measurements of contact (θ) and sliding-angles (α) with water. Work of adhesion (W) and interaction energies were subsequently calculated by using the values of θ and α, respectively. For the evaluation of actual performances of polymeric materials, shear strength of ice adhesion and snow accretion were measured. Characteristics of homogeneous surfaces of polymers in the interaction with water were obtained. On the basis of these concepts, the materials with heterogeneous surfaces were synthesized. Results of surface characterizations in these polymers showed that the relationships between θ and α, and the other surface attributes are very different according to polymer systems. The surface controlled energetically and morphologically, and the superior hydrophobic property prevented the snow accretion, but not ice adhesion. On the other hand, the organopolysiloxane modified with lithium compound provided the lowest strength of ice adhesion, but a poor capability of snow repellency. In the structural and energetic viewpoints', interactions between heterogeneous surfaces and water (snow and ice) were discussed. For the theoretical prediction, the intermolecular energies between model polymers and water were calculated by using a molecular orbital SCF method. The order of interactions calculated were coincident with experimental values deduced from α, but not from θ. The advantage of heterogeneity of surface was supported by the theoretical understanding. © 1994 John Wiley & Sons, Inc.

INTRODUCTION

Hindrances caused by snow accretions and ice adhesions in cold atmospheres often result in accidents involving human life. In the field of navigation, aviation, and others, such materials, which prevent or mitigate ice and snow adhesion, have been wanted for a long time. Numerous attempts by using various materials have been discussed in publications.[1-3] Applications of typical polymers having low critical surface tension, like organopolysiloxane and polytetrafluoroethylene, were unsuccessful. The authors investigated the mechanism of ice adhesion and snow accretion fundamentally, and some of the new aspects dominated interactions with water, snow, and ice. As known in the biomedical composite materials, heterogeneous surfaces consisting of multiphase system provide more characteristic performance than homogeneous surfaces from single-phase system. The thesis is to elucidate how the heterogeneity influences the reduction of the interaction with water.

EXPERIMENTAL PROCEDURE

To investigate the mechanism of interactions between polymeric materials and water (ice, snow), test and evaluation methods are described as follows.

Test and Evaluation Methods

Measurements of Contact Angle (θ)

Contact angles formed between film surface and water droplet, as the characteristic of the static interaction in thermodynamic equilibrium in the wa-

* To whom correspondence should be addressed.

Journal of Applied Polymer Science, Vol. 54, 2051-2062 (1994)
 CCC 0021-8995/94/132051-12

ter/polymer system, were measured in the air and also in a hydrophobic medium by a goniometer (Kyowa Kaimenkagaku Co. CA-S), which consists of a contact-angle meter, TV monitoring system, and circulating bath for temperature regulation, at 293 and 258 K (in the states of super-cooled and icing). For the water droplet, distilled deionized water was used, 50 μL in volume. Size of test pieces was 25 × 8 mm.

Calculation of Work of Adhesion ($W - \pi_e$, W)

Interaction energies between material surface and water (ice) were calculated as the specific work of adhesion of water (ice) ($W - \pi_e$) against polymer by using the values of contact angle (θ) measured in the air. The $W - \pi_e$ can be calculated by the correct form of the Young-Dupré[4] modified by Bangham and Razouk[5]:

$$W - \pi_e = \gamma_w(1 + \cos\theta) \quad (1)$$

where γ_w is the free surface energy of water, θ is contact angle of water/substrate and π_e is the reduction in surface energy of the solid due to adsorption of vapor from liquid being measured. When contact angles of water droplet on a substrate are measured in hydrophobic medium, e.g., in liquid paraffin, then π_e can be eliminated and intrinsic work of adhesion W obtained[6]:

$$W = \gamma_w(1 + \cos\theta_1) + \gamma_p(\cos\theta_1 + \cos\theta_2) - 2(\gamma_w^d\gamma_p)^{1/2}\cos\theta_1 \quad (2)$$

where γ_w, γ_p, and γ_w^d are free surface energies of water (ice), paraffin, and dispersion component of water (ice), respectively. The θ_1 and θ_2 are contact angles of water (ice)/substrate in paraffin and that of paraffin on the same substrate, respectively. To solve the eqs. (1) and (2), free surface energies and entropy of temperature must be available. On the base of values obtained by Fowkes[7] and Hobbs,[8] dispersion and hydrogenbond components of free surface energies in the water/ice system were calculated. Schematic representation of these relationships is shown in Figure 1. With this figure total free surface energies in water/ice system at arbitrary temperature can be calculated. The π_e will be obtained from the difference $W - (W - \pi_e)$.

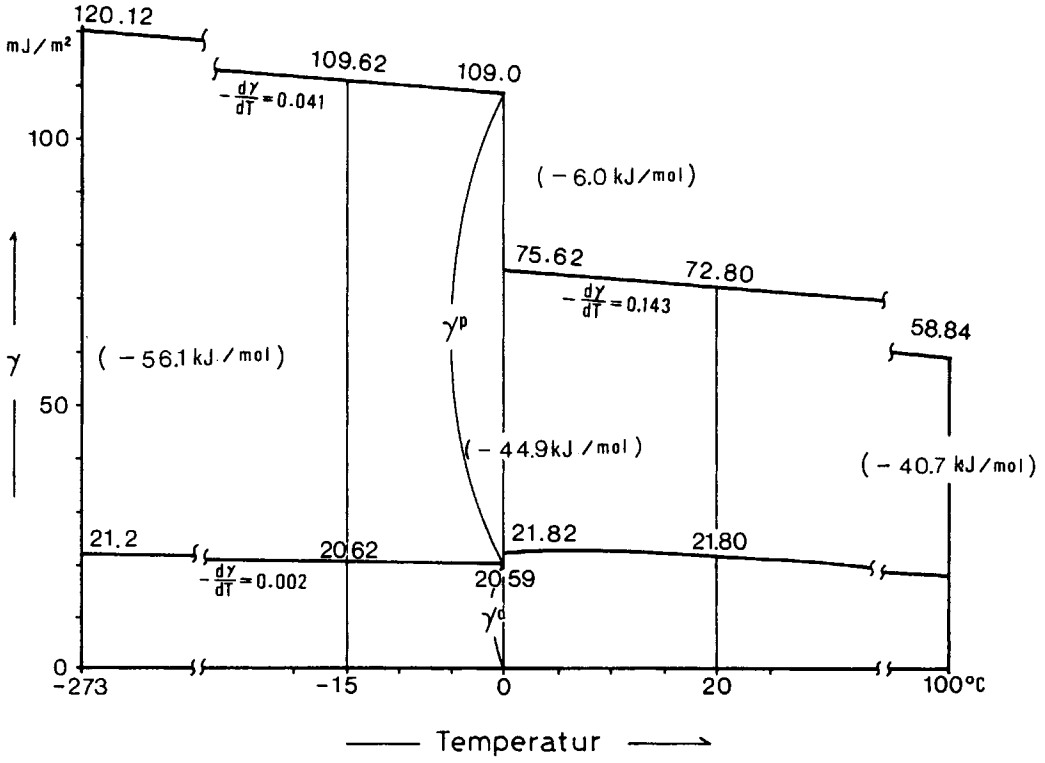

Figure 1 Dispersion and hydrogen bond components of free surface energies of water and ice.

Measurements of Sliding Angle (α)

Sliding angle α is so defined as the critical angle, in which liquid droplets with a certain weight begin to slide down on the inclined plate,[9] and characterizes the dynamic interaction in liquid/solid interface. Measurements were made by using the simple apparatus derived by us. The other conditions were same as for contact angles. The quantity of water droplets varied between 3–100 mg. Size of test pieces was 100 × 100 mm.

Calculation of Interaction Energies

For the measurements of interaction energies between the surface of polymers and water, the following equation is established. If the deformation and moment of rotation were ignored, the following relationships would be available:

$$2\pi r E d = mg \cos \alpha \tag{3}$$

$$r = R \sin \theta \tag{4}$$

where R and r are radii of water droplet and contact circle, and θ and α are contact- and sliding-angle, respectively. And m is weight of droplet, g is gravitational acceleration, E is the interaction energy of unit area, and d is effective width of the surface layer. Here, d is regarded as the size of 1 molecule of water, i.e., 5×10^{-8} cm.[10] Simultaneous equations with (3) and (4), using the relationship $\frac{4}{3}\pi R^3 \rho g = mg$ (ρ: specific weight of water), led to the following relationship, by which the interaction energy E can be calculated:

$$E = \frac{(3\ mg)^{2/3}\rho^{1/3}\cos \alpha}{6\pi^{2/3} d \sin \theta} \times (2 - 4 \cos \theta - \cos^2\theta + \cos^3\theta)^{1/3} \tag{5}$$

Measurements of Adhesive Forces of Ice (F)

For the evaluation of adhesive forces of ice, the test device made by us was used, which consists of temperature-regulated chamber, process controller, load cell, and recorder. The stainless-steel metal ring with inside section area 5 cm^2, height 1.5 cm, was set on polymer surface of test plates and precooled for 90 min at the predetermined temperature; then, 2 mL of distilled deionized water stored at 278 K was poured into the ring. After 3 h at that temperature, shear strength of ice adhesion was measured. Substrate of test pieces made of stainless steel was 70 × 90 × 10 mm in size.

Measurements of Snow Accretion

Experiments were conducted in a cold wind tunnel (Göttingen type) at the Institute of Low Temperature Science, Hokkaido University, by using natural snow stored at 253 K. The behavior of snow repellent efficiency was investigated by varying temperature (273 K, 270 K), wind speed (5–20 m/s), and snow density (0.4–0.6 g/cm^3). Dimensions of test panels were 150 × 50 mm.

INTERACTIONS BETWEEN HOMOGENEOUS SURFACES OF POLYMERS AND WATER (SNOW, ICE)

Materials

Polymeric materials used in this investigation are listed in Table I. Resins 1–10 were coated by solidification from solution on the plates in the sizes adapted to each test method described above. Plastic plates 11–21 were cut into the test panels in the same sizes above and were adhered to the stainless-steel plates with 10-mm thickness only for the measurement of shear forces of ice.

Results and Discussion

The values obtained for contact angles of super-cooled water at 258 K in the air were in most cases smaller than that of water at 273 K. They went down after icing. A possible explanation for this is the very strong momentary interaction of super-cooled water molecules with the adsorbed ones on icing, whereas contact angles measured in paraffin were not so characteristic. The values of W and $W - \pi_e$ of various polymers are shown in Figure 2. The π_e were obtained by the eliminating of W, i.e., from the difference $W - (W - \pi_e)$. As can be seen, π_e values are negative with a few exceptions, although from a theoretical view point these must take positive values. It has been revealed that the value for π_e ignored by Landy and Freiberger[11] can be evaluated by this method. Figure 3 shows the dependence of sliding angles on the weights of water droplets in several polymers. The θ of PTFE (polytetrafluoroethylene) and PP (polypropylene) are 104.3° and 96.4°, respectively, while α of PP is lower than that of PTFE. In comparison with PFAA (polyperfluoroalkylacrylate) and PDMS (polydimethylsiloxane), θ are 117.0° and 95.8°, respectively, α for PDMS is much lower than that of PFAA; therefore, water droplets slide more easily on the PDMS than PFAA. In general, it is believed that interactions

Table I Polymeric Materials Used in This Investigation

No.	Abbrev.	Polymers	Manufacturers	Products
1	IBM	Poly-i-butylmethacrylate	Mitsubishi Rayon	BR-101
2	NBM	Poly-n-butylmethacrylate	Mitsubishi Rayon	LR-1215
3	MMA	Polymethylmethacrylate	Mitsubishi Rayon	BR-85
4	PST	Polystyrene	Mitsubishi Monsanto	HH-103
5	PES	Polyester	Nihon Gosei	220
6	VAC[a]	Polyvinylacetate-chloride	Union Carbide	VAGH
7	PFA[b]	Polyperfluoroacrylate	Kansai Paint	PFAA
8	SH	Organopolysiloxane	Toray Dow Corning	SH-237
9	SIO	Organopolysiloxane	Toray Dow Corning	PRX-305
10	PUR	Polyurethane	Kansai Paint	PG-80
11	PVC	Polyvinylchloride	Takiron	604
12	PCB	Polycarbonate	Asahi Glass	Lexan
13	PHE	Phenol resin	Matsusita Electric	R7140
14	N-6	Nylon 6	Toray	CM-1017
15	NYL	Nylon 66	Toray	CM-300 1N
16	ACT	Polyacetal	Mitsubishi Eng. Berlin	—
17	PE	Polyethylene	Shin-Kobe Electric	P-sheet EL
18	PP	Polypropylene	Shin-Kobe Electric	Enpla
19	TFE	Polytetrafluoroethylene	Nippon Valqua	Valflon
20	FEP[a]	TFE-ethylene copolymer	Asahi Glass	Aflon COP
21	SPF	Solid Paraffin	Wako Pure Chem.	MP 341-343K

[a] Exceptional samples (copolymers).
[b] Almost homopolymer.

will decrease with increasing contact angle. However, the reversal in θ and α in these cases was very significant. Some relationships between W and F can be seen. The minimum of ice adhesion was found on the polymer organopolysiloxane. The value amounted to about 10^2 kN/m^2. Analysis of the results suggested that the glass transition temperature (T_g) together with low surface energy must relate

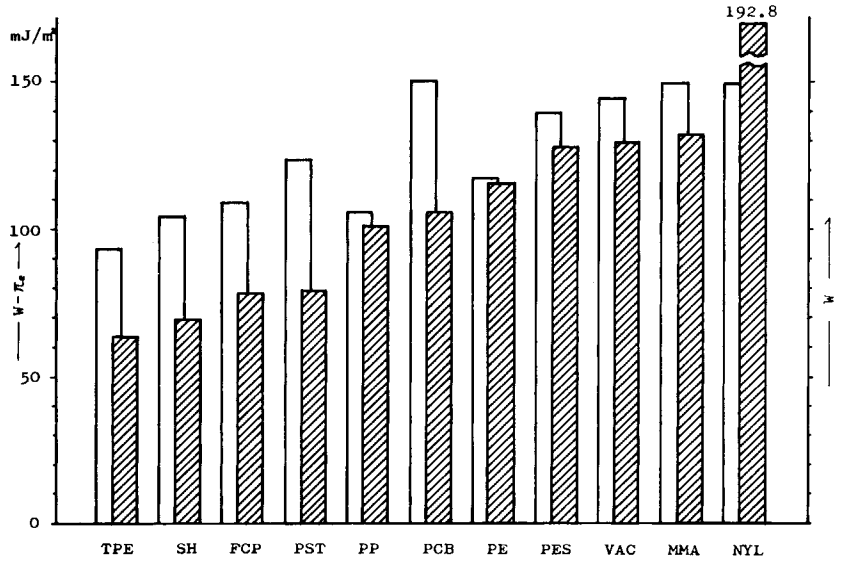

Figure 2 Comparison of work of adhesion W with $W - \pi_e$ between polymers and ice at 258 K.

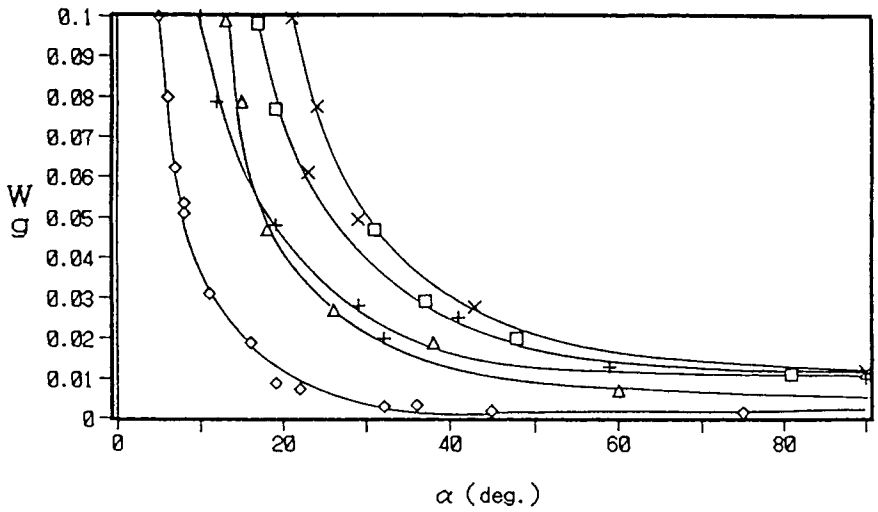

Figure 3 Dependencies of sliding-angles on the weights of water droplets in several polymers. (□) PTFE; (+) PFAA; (◇) PDMS; (△) PP; and (×) PUR.

to mitigate ice adhesion. Three-dimensional representations of W in the air at 258 K, T_g, and adhesion forces (F) for various polymeric materials are shown in Figure 4. As can be seen in the figure, minimizing of ice adhesion exists in the field of minimum W and T_g (Field A). Organosiloxane polymers belong to this field. The outstanding fact was that FEP (ethylene–tetrafluoroethylene copolymer) has a lower value for F than both of PE and PTFE. Another possibility for lower ice adhesion is in the field of relative higher W and T_g. The polymers are PCB (polycarbonate), NYL (nylon 66), and PHE (phe-

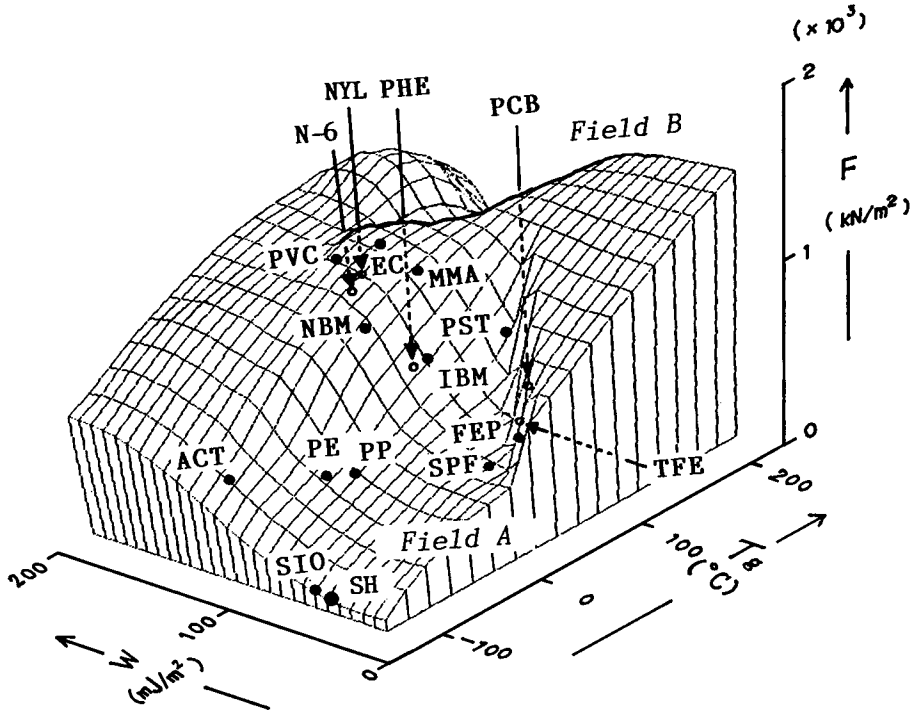

Figure 4 Three-dimensional diagram for the work of adhesion (W), adhesive strength of ice (F) at 253 K, and glass-transition temperature (T_g).

nol) (Field B). Something in common with these polymers in this field is that they have absorbed water molecules in them. Nothing under these homogeneous surfaces of polymers, including some exceptional copolymers, prevented snow accretion.

INTERACTIONS BETWEEN HETEROGENEOUS SURFACES OF POLYMERS AND WATER (SNOW, ICE)

As shown in the previous section, typical polymer materials having low surface energies, such as polymers with saturated alkyl group, organopolysiloxane, and perfluoroalkyl groups showed higher hydrophobicity and substantially lower adhesive strengths of ice in comparison with conventional polymers. The trials with these materials, however, could not help to prevent the adhesion of water droplet, ice, and snow accretion. It seemed difficult to realize the expected properties with a homogeneous surface composed of single-phase polymer. Further investigations proceeded with heterogeneous surfaces.

Materials with Heterogeneous Surfaces

Numerous attempts according to the findings obtained in the fundamental investigations of interactions between polymer surfaces and water, snow, and ice have led the developments of the following three types of composite materials with heterogeneous surfaces, which remarkably reduce the relevant interactions[12]:

Organopolysiloxane Modified with Lithium Compound (Symbol: S III)

This material was composed essentially of organopolysiloxane prepolymer and lithium compound. Polymerization system of binder is shown in eqs. (6) and (7):

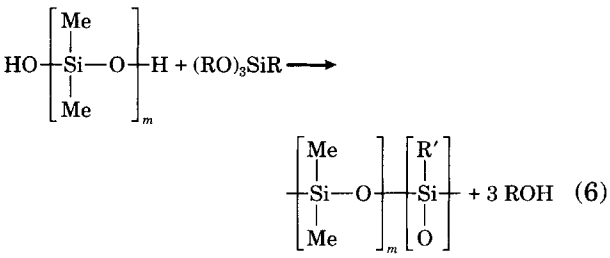

$$LiMO_3 + 2\,ROH \longrightarrow 2\,LiOR + MO_2 + H_2O \qquad (7)$$

where R, R' are alkyl groups, m and n are repeat units of monomer, respectively, and M is an element of IV group. Equation (7) shows reaction system between by-product from reaction (6) and lithium. Both reactions proceed simultaneously, and heterogeneous structure of this composite material is formed during film formation.

Organopolysiloxane Grafted Fluoro Polymer (Symbol: FX)

The copolymer can be synthesized by the grafting between organopolysiloxane macromonomer having a NCO-functional end-group and polyfluoro-olefin having hydroxyl group. Chemical structure is shown in the following:

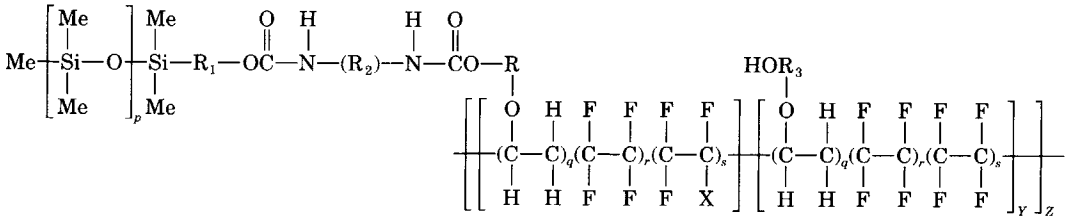

(8)

where R_1, R_2, and R_3 denote saturated hydrocarbon residuals; X is halogen; p, q, r, and s are the numbers of each monomer units; and Z is the number of branched polymer chains. Hardening is induced by additive reaction of multifunctional isocianate group to the residual hydroxyl group in the main chain.

Polyperfluoroalkyl(meth)acrylate Combined with Hydrophobic Silicium Dioxide (Symbol: NX)

Base polymer is synthesized by radical polymerization of a perfluoroalkyl(meth)acrylate- and meth-acryloxy-comonomer having multifunctional alkoxyvinylsilane group. Chemical structure of the copolymer can be represented as follows:

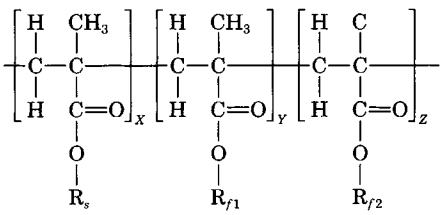

(9)

where R_a, R_{si}, and R_{pf} are alkyl, alkoxysilane, and perfluoroalkyl groups, and k, l, m, and n are the number of repeated monomer units, respectively. Hardening system is self-crosslinking of alkoxy groups in the presence of atmospheric moisture. Chemical and morphological heterogeneity can be produced by the addition of hydrophobic silicium dioxide, which is made by surface modification with dimethyl-disilazane.

Results and Discussion

It was found that ice adhesion can be almost completely prevented by the composite material (S III). The value of ice-adhesion strength against this material amounted to about 10 kN/m^2, and could not be realized in the homogeneous polymer system. XRD (X-ray diffraction) and pulsed-NMR (nuclear magnetic resonance) analyses detected that the octahedron coordination from Li ion, carboxylate group, and water molecules was formed, and the presence of bound and restrained water molecules, respectively. Structural and energetic differences and synergetic effects from silicone matrix resulted in preventing ice adhesion. Because of incompatibility between backbone and substituted segments, the copolymer (FX) has a phase-separated structure, so-called "sea-island," which corresponds to backbone-substituted chains. Mechanical strength of this film is much stronger than that of S III, due to the rigidity of fluoro-polymers' backbone. Adhesive strength of ice to the surface of the copolymer decreased with increasing grafting. At the molar ratio 0.05 of macromer/backbone, energy of ice adhesion was minimized to about 10^2 kN/m^2, about half the value of PTFE and considerably lower than polyvinylfluoride and polyvinylidenefluoride. Contact angle of the surface with water was a little lower than that of PTFE; sliding-angle, however, was much lower compared with the latter. The surface of the material (NX) is characterized in the lowest free surface energy under 10 mJ/m^2, high hydrophobicity (contact angle 117°). Dispersion of a hydrophobic silicium dioxide with the radii of particles 0.1–0.01 μm to this matrix (F/M ratio = 2.0) remarkably improved its hydrophobicity and repellent attribute against water droplet. Measured contact- and sliding-angle are 156° and 5° (8.0 mg), respectively; whereas 117° and 5° (400 ~ 640 mg) for base copolymer of PFAA, and 104° and 5° (1,000 mg) for PTFE, respectively. Dependencies of the weights of water droplets on sliding-angle for the three types of materials are shown in Figure 5. Contact-angles, sliding-angles, W of ice and snow accretion of these polymers compared with that of PTFE are summarized in Table II. From this table it is obvious that even material with the lowest ice adhesion cannot prevent snow accretion, while the material having anti-snowing attribute don't mitigate the strength of ice adhesion. Anti-snowing attribute requires some other aspects of ice-adhesive strength. The findings of relevant experiments showed that

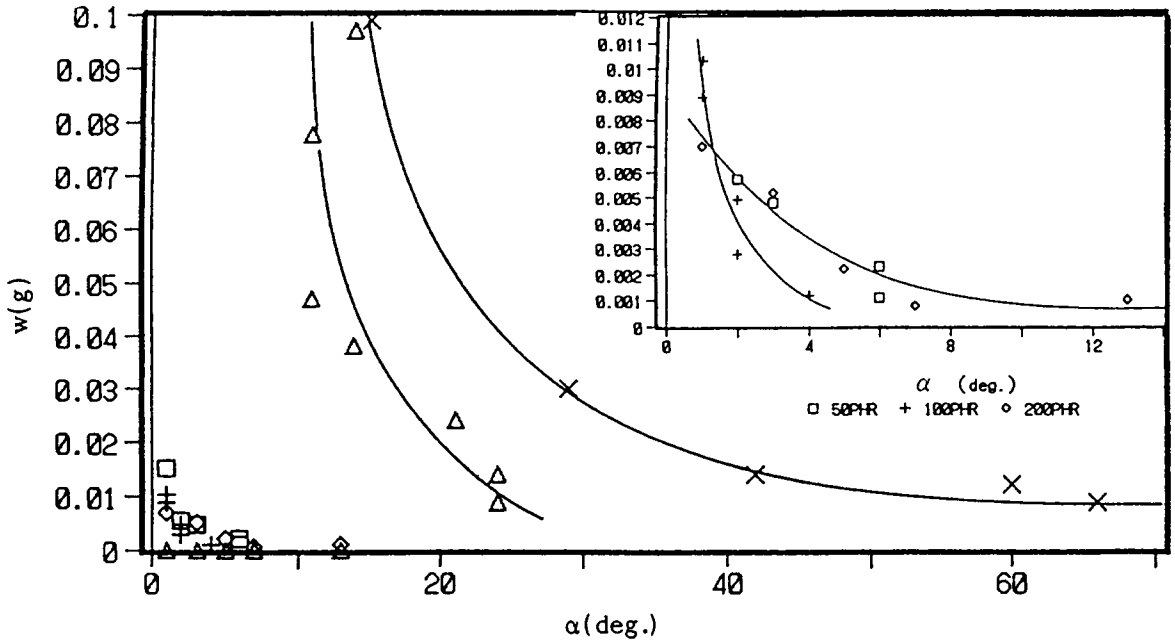

Figure 5 Relationships between sliding-angles and weights of water droplet. (□) NX; (△) FX; and (×) S III.

Table II Surface Characteristics of the Heterogeneous Materials in Comparison with Polytetrafluoroethylene

Materials	S III	FX	NX	PTFE
Contact-angle (degree) (293 K)	104.0	100.5	156.0	104.6
Sliding-angle (degree) (m = 50 mg, 293 K)	21.7	13.5	2.5[a]	26.3
Work of adhesion ($W - \pi_e$, mJ/m^2)	97.2	119.2	19.8	93.8
Ice adhesion (10^2 kN/m^2 258 K)	0.1	0.8	0.5–2.0	2.5
Snow accretion (g/cm^2)[b]	0.08	0.04	0.00	0.15

[a] Weight of water droplet: 5 mg instead of 50 mg.
[b] Specific weight of snow: 0.44; wind speed: 10 m/s.

snow accretion tended to decrease with the increasing water contact-angle formed between material and water. Snow has a considerably smaller specific gravity (0.03–0.60) than ice; therefore it adheres and accumulates to the objects more easily, even though the interaction energies between substrates and snow are very low. Wet snow contains water in itself and is called "sherbet-like." Snow accretion in this state occurs easier at atmospheric temperatures in the vicinity of 273 K than "dry" snow at lower temperature below 270 K. Experiments by Mizuno et al.[13] showed that the strength of snow adhesion increases with its water contents, and the highest values were observed at 12 ~ 16%. This water contributes to the adhesive force between substrates and snow when contact of snow to the object happens, even though before icing. In contrast to snow, the phenomenon of ice adhesion is characterized when the phase changes from liquid water to solid. The motive force for adhesion is the strong interaction due to hydrogen-bonding between substrate and ice.

INVESTIGATION OF INFLUENCE OF CHEMICAL STRUCTURES IN THE INTERACTION WITH WATER

To investigate the relationships between chemical structures of polymer surfaces and the interaction with water, the following experiments were made.

Materials

Two kinds of typical hydrophobic polymeric materials, i.e., polyperfluoroalkylacrylate (PFAA) and polydimethylsiloxane (PDMS) were used. For details of these polymers, see the previous section. To control surface morphologies, hydrophobic filler was dispersed in each polymer matrix by varying F/M ratios 0.0–3.0. Coating compositions were applied by doctor blade on the aluminum plates (100 × 100 × 1 mm) treated with chromium phosphate, and dried for 60 min at 373 K and 1 wk at ambient temperature. Average thickness of dry film amounted to 10.0 + 1.5 μm.

Characterization

Contact- and sliding-angles were measured according to the methods described. Chemical structures of the surfaces in both systems were analyzed by XPS (X-ray photoelectron spectroscopy, Simadzu Co., ESCA750), and surface roughness was measured by surface roughness tester (Tokyo Seimitsu Co., SURFCOM 550).

Results and Discussion

The relationships between contact-angles, sliding-angles, and filler/matrix ratio (F/M) in PFAA and PDMS systems are shown in Figures 6 and 7, respectively. It is noticeable that PFAA and PDMS without filler (only binder) are antagonistic in the contact angles and sliding angles. The θ and α in 10 mg in PFAA system are inversely proportion to the contact angle, while in the PDMS system the relationship between θ and α is conspicuous. The former has 117 of θ and 90 of α in 10 mg of droplet, whereas the latter has 96 of θ and 18 of α in the same weight. Contact angle of PFAA increases with increasing F/M ratio. From the ratio 0.15 θ becomes rapidly higher and maximum value 156 (F/M = 0.25). On the other hand, contact-angle of PDMS increases gradually with increasing F/M ratio, and maximum

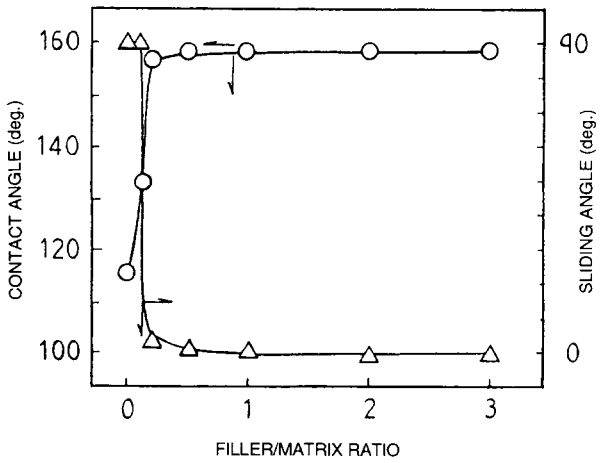

Figure 6 Relationships between contact-angles and sliding-angles, and filler/matrix ratio in the PFAA system.

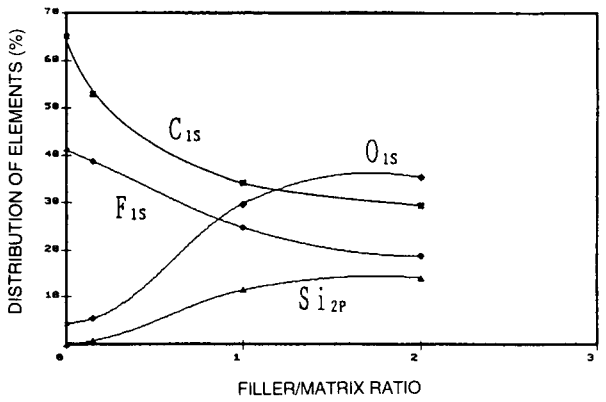

Figure 8 Relationships between filler/matrix ratios and distributions of elements in the PFAA surface measured by XPS.

value 148 is observed in the ratio 3.0. The α in the cases of films *without* and *with* filler in lower concentration (F/M ratio = 0.5) are very low, and maximum value for α exists in the vicinity of 1.0 in the F/M ratio. Discrepancy between θ and α in PFAA and PDMS systems must result from different interactions of chemical species of surface with water. To explain these phenomena in the viewpoints of chemical structures, analyses by XPS were carried out. Results are shown in Figures 8 and 9, respectively. Si_{2p} and O_{1s} *increase,* and F_{1s} and C_{1s} *decrease* with increasing F/M ratio. That means that atoms Si and O originated from hydrophobic silicium dioxide exposed on the surface of the film. On the other hand, Si_{2p} in the PDMS system is concentrated about 2 times more than in the PFAA system; however, it depends a little on the F/M ratio. Si_{2p} is not distinguished whether of binder (PDMS as matrix) or filler. Decrease of C_{1s} and increased O_{1s} with increasing F/M ratio also suggest that exchange of matrix with filler on the surface takes place. Surface roughness of both films is shown in Figure 10. The value 1 for F/M ratio is nearly coincident in both systems. The differences in the interactions, therefore, will be deduced from surface chemical structures, namely, the surface of PDMS system is covered with a single chemical group, i.e., $-CH_2-$, $-CH_3$ from binder and filler. In contrast, the surface of the PFAA system is distributed with different chemical segments, i.e., $-CH_2-$, $-CH_3$, $-CF_2-$, and $-CF_3$. The former can be called "homogeneous" and the latter "heterogeneous" chemical sites. The ultrahydrophobic surface can be obtained by the synergetic effects from an heterogeneous chemical structure and morphology. These findings lead to

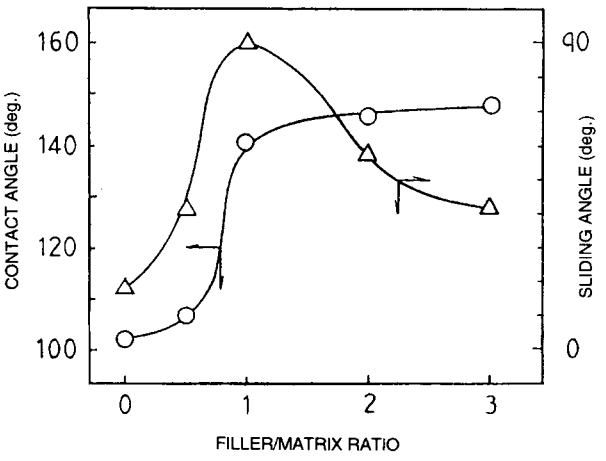

Figure 7 Relationships between contact-angles and sliding-angles, and filler/matrix ratio in the PDMS system.

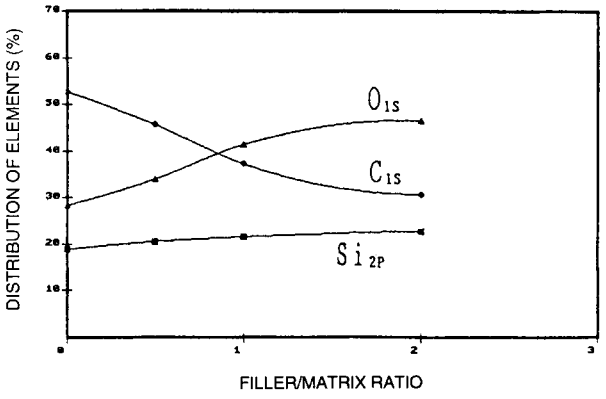

Figure 9 Relationships between filler/matrix/ratio and distribution of elements in the PDMS surface measured by XPS.

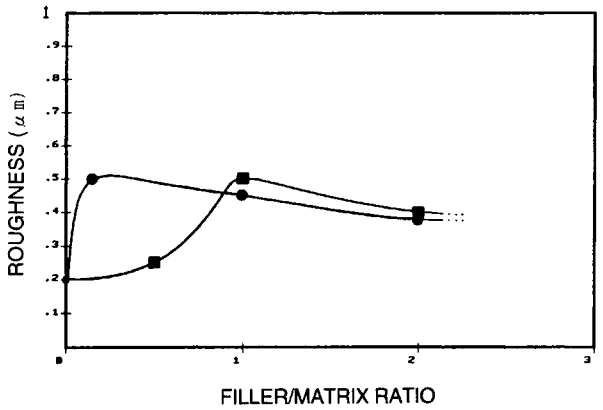

Figure 10 Influences of the filler/matrix ratios in the surface roughness in PDMS and PFAA systems. (●) PFAA system; (■) PDMS system.

the conclusion that the heterogeneities of surface can contribute to decrease the interaction energies with water, and increase hydrophobicity, and consequently counteract snow.

CALCULATION OF INTERACTION ENERGIES BETWEEN HYDROPHOBIC MATERIALS AND WATER BY MOLECULAR ORBITAL METHOD

As previous experiments showed, behavior of hydrophobic polymers against water are very different from each other from a microscopic viewpoint. Materials characterized as nonpolar molecules comprise saturated linear hydrocarbons, fluorocarbons, and organosiloxane groups. For the theoretical prediction of the phenomena at the molecular level, interaction energies between these polymers and water were calculated with the help of quantum chemistry.

Model Polymers

Three types of modeling molecules were selected:

1. Hydrocarbon (LHC): ethane C_2H_6
2. Dimethylsiloxane (DMS): $CH_3 - \{(CH_3)_2Si\}_4 - Si(CH_3)_3$
3. Hexafluoroethane (FHC): C_2F_6.

Method

For the calculation of molecular orbital energies MOPAC version 6.01, PM3 was used, by which interactions can be assessed by the semi-empirical SCF method in the state of structural optimization.

Results and Discussion

Data obtained are shown in Table III. Distances between polymers and water molecule are 0.187 nm for FHC/water system, 0.252 nm for LHC/water system, and 0.329 nm for DMS/water system. In comparison with interaction between the nearest atoms of molecules, i.e., oxygen from H_2O and hydrogen from DMS, the energies are a little larger energies than that of LHC. On the other hand, in interaction energies between O or H atom of water and whole DMS molecule, the former are attractive and the latter are repulsive. In the case of FHC/

Table III Interaction Energies Between Hydrophobic Polymers and Water Calculated by SCF Method

Interaction Forms		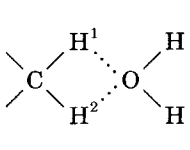	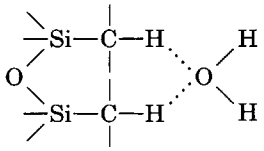	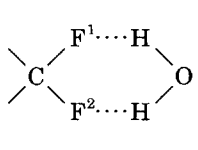
Bond length (nm) (OH, FH)		0.252	0.329	0.187
Interaction energies (kJ/mol)	E_1^1	−14.95	−15.64	−50.89
	E_1^2	−5.70	−12.30	−48.51
	E_2	−4.07	−4.64	−0.40
	E_3	−0.81	+1.75	−39.89
	E_4	−1.40	+1.79	−35.81

E_1: $O_{H_2O} - H_{HC,DMS}F_{FHC} - H_{H_2O}$.
E_2: $O_{H_2O} - mol_{HC,DMS}$.
E_3, E_4: $H_{H_2O} - mol_{HC,DMS,FHC}$.

Table IV Comparison of Characteristics of Three Types of Hydrophobic Polymers

Polymers	PPC	PDMS	PFAA
Contact-angle (θ) (degree)	96	102	117
Surface tension (mN/m)	31.8	23.0	11.8
Work of adhesion (mJ/m^2)[a]	65.19	57.66	39.75
Sliding-angle (α) (degree)	20.0	20.0	20.0
Weight of droplet (g) (α = 20°)	0.042	0.012	0.046
Interaction energies (mJ/m^2)[b]	22.66	10.49	30.49
	LHC	DMS	FHC
Interaction energies (mJ/m^2)[c]	14.95	15.64	50.89
Interaction energies (mJ/m^2)[d]	6.28	1.10	75.90

[a] Calculated by eq. (1).
[b] Calculated by eq. (5).
[c] SCF method (E_1^1).
[d] SCF method ($E_2 + E_3 + E_4$) from Table III.

water system, interaction energies between F and H are about 3 times that of DMS. Interactions between H of water and FHC molecules are also have large, attractive potential. These calculated values of fluoropolymers explain a relatively strong adhesion with water and a large sliding-angle, but not a large contact-angle. It is known that the contact of LHC with water enhanced the structural conformation, build-up "iceberg" structures.[14] The negative excess entropy in the interaction between hydrophobic surface and water results in high hydrophobicity.[15] The effect of negative entropy can be expected in other model polymers. From the structural analogy, the model polymers LHC, DMS, and FHC can be nearly compared to the polymeric materials PP, PDMS, and PFAA, respectively. For the comparison of predicted with observed interactions, energies were calculated with eq. (5). The interaction energies thus measured for the three types of hydrophobic polymers are listed in Table IV in comparison with intermolecular energies calculated by SCF method and by contact-angle method (work of adhesion). On the polymer of PFAA, the term negative entropy overcomes interaction energies (enthalpy), so that interactions between clustered water molecules and PFAA molecules decrease. This is the reasoning of a large value for θ, and make it apparently high hydrophobicity. Contact area of water droplet on PFAA, therefore, decreases; however, adhesion energies still remain larger than PDMS and LHC because absolute interaction energies of PFAA in the unit area are large. The values of work of adhesion derived from static measurements of contact-angles are ordered as PP > PDMS > PFAA. On the other hand, among the interaction energies obtained from sliding-angle, PDMS has the smallest value, and PFAA has a value about 3 times that of PDMS. This ratio is exactly coincident with the data predicted by theoretical one (SCF method E_1^1). The order of total interaction energies between the whole polymers and water molecule ($E_2 + E_3 + E_4$) also corresponds to the observed one from α, namely, PFAA > LHC > PDMS. This means that the order obtained from θ is reverse to that from α. The fact that organopolysiloxane has an advantage over perfluoropolymer to repel water droplet is consistent with the tendency of intermolecular energies predicted by the molecular orbital method, but not with interaction energies obtained by contact-angles.

TRIAL OF CALCULATION FOR HETEROGENEOUS SURFACES

Calculation for the heterogeneous system in surface by using a single model was attempted. Intermolecular energies between both segments from FHC and DMS and water molecule were calculated. Results are shown in Table V. It is noticeable that the energies decrease when both sites of FHC and DMS molecules close into a water molecule. Interaction energies between H atoms from DMS and O atom from H_2O, and especially between F atoms from FHC and H atoms from H_2O decrease in comparison with the values of single segment of polymers. Results will suggest the conformation of different segments, i.e., heterogeneous chemical sites of surface decrease the interaction with water. These theoret-

Table V Interaction Energies Between DMS, FHC, and Water Calculated by SCF Method

Interaction Forms	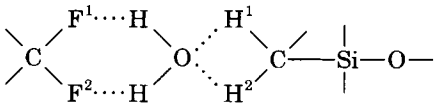			
Bond length (nm)	(F—H)	0.307	(O—H)	0.267
Interaction energies (kJ/mol)	E_1^1	−10.28		−9.60
	E_1^2	−13.62		−7.58
	E_2	−0.94		+2.41
	E_3	−0.32		−5.00
	E_4	−2.58		−2.07

E_1: $F_{FHC} - H_{H_2O}$, $O_{H_2O} - H_{DMS}$.
E_2: $O_{H_2O} - mol_{DMS}$.
E_3, E_4: $H_{H_2O} - mol_{FHC}$.

ical predictions supported experimentally verified profitability of heterogeneity. Illogicality of difference in dimensions between intermolecular (nm) and domain size of phase-separated polymer surface (μm) can be explained that the negative entropy influencing the clusterization of water molecules should act a microscopic intermolecular interaction (short-range force) to a macroscopic range. These types of the heterogeneous surfaces of polymers developed by us empirically are just included in this category.

CONCLUSION

Heterogeneous components and structures provide characteristic surface properties, especially in the interaction with water. New materials which decrease interaction with water were developed. The mechanisms for the mitigation of intermolecular interaction were substantially elucidated by the experimental investigations and also theoretical predictions. Further investigations for the advanced performances of the materials must be proposed to interpret the relationships between structures and functions in molecular levels, i.e., what kind of chemical heterogeneity and what order in sizes between nm and μm should minimize the relevant interactions. For the theoretical supporting the calculation system by quantum chemistry will play a more important role.

The authors acknowledge valuable suggestions and support by the Japan Civil Aviation Bureau, Ministry of Transport, and the Institute of Low Temperature Science, Hokkaido University.

REFERENCES

1. G. H. Ahlborn, U. S. Environ. Protection Agency, *Report EPA-600,* 1976, pp. 1–203.
2. L. D. Minsk, U. S. Army Corp. of Engineering, *Special Report,* 1985, pp. 8–28.
3. V. K. Croutch and R. A. Hartley, *J. Coatings Technol.,* **64,** 41–53 (1992).
4. H. W. Fox and W. A. Zisman, *J. Colloid Sci.,* **5,** 514–531 (1950).
5. D. H. Bangham and R. I. Razouk, *Transactions of the Faraday Society,* **33,** 1459 (1937).
6. H. Murase and K. Nanishi, *Ann. Glaciology,* **6,** 146–149 (1985).
7. F. M. Fowkes, *Attractive Forces at Interface, Industrial and Engineering Chemistry,* **56,** 40 (1964).
8. P. V. Hobbs, *Ice Physics,* Clarendon Press, Oxford, 1973.
9. J. J. Bikerman, *J. Colloid Sci.,* **5,** 349 (1950).
10. K. Itagaki, *Physicochemical Aspects of Polymer Surfaces,* Vol. 1, Flonum Publishing Corp.
11. M. Landy and A. Freiberger, *Studies of Ice Adhesion, Colloid and Interfacial Science,* **25,** 231–244 (1967).
12. H. Murase, K. Nanishi, and H. Kogure, *X IX FATIPEC Congress Book,* Vol. IV, 1988, pp. 203–222.
13. Y. Mizuno and G. Wakahama, *Low Temperature Science, Physical Edition,* Vol. 35, Sapporo, 1977, pp. 133–145.
14. R. B. Herrmann, *J. Phys. Chem.,* **75,** 363 (1971).
15. G. Nemethy, *Angewandte Chemie,* **79,** 260–271 (1967).

Received April 1, 1994
Accepted June 15, 1994